Chemically reacting on MHD boundary layer flow of CuO-water and MgO-water nanofluids past a stretching sheet in porous media with radiation absorption and heat generation/absorption

To cite this article: E Kumaresan *et al* 2017 *IOP Conf. Ser.: Mater. Sci. Eng.* **263** 062017

IOP Conf. Series: Materials Science and Engineering **263** (2017) 062017 doi:10.1088/1757-899X/263/6/062017

Chemically reacting on MHD boundary layer flow of CuO-water and MgO-water nanofluids past a stretching sheet in porous media with radiation absorption and heat generation/ absorption

E Kumaresan, A G Vijaya Kumar and B Rushi Kumar
Department of Mathematics, School of Advanced Sciences, VIT University, Vellore-632014, Tamil Nadu, India

E-mail:vijayakumarag@vit.ac.in

Abstract. In the present investigation, a numerical analysis has been carried out for steady two dimensional MHD free convective boundary layer flows of electrically conducting nanofluids past a uniformly stretching sheet through porous media with radiation absorption, heat generation/absorption, thermal radiation, chemical reaction, thermo-diffusion and diffusion – thermo effects. We considered two types of nanofluids namely MgO -water and CuO -water. The mathematical model was governed by a system of linear and non-linear partial differential equations with prescribed boundary conditions. The governing boundary-layer equations are first transformed into a system of coupled nonlinear ordinary differential equations using similarity variables. The transformed equations were solved numerically by the shooting method with Runge-Kutta scheme. Finally the effects of various dimensionless governing parameters like magnetic field parameter, chemical reaction parameter, thermal radiation parameter, radiation absorption parameter, heat generation parameter, Dufour number, Soret number, volume fraction of the nanoparticles and shape of the nanoparticles on velocity, temperature and concentration profiles along with the friction factor, local Nusselt and Sherwood numbers are thoroughly studied and explicitly explained in tabular form.

Nomenclature.

M Magnetic parameter
C_P Specific heat constant pressure
C_W Uniform constant concentration
K Permeability parameter
D_2 Mass diffusion coefficient
q_r Radiative heat flux
T_w Uniform constant temperature
k_0 Rate of chemical reaction
Q_0 Dimensional heat absorption
Q Heat absorption
Q_1 Radiation absorption parameter
Ec Eckert number
C Concentration of the species
N Radiation parameter
D_m Species diffusivity
Nu_x Nusselt number

v Velocity in the y - direction
u Velocity in the x -direction
(x, y) Cartesian coordinates
D_1 Temperature diffusion coefficient
k_s Thermal conductivity of nanoparticle
C_∞ Free stream concentration
Du Dufour number
Pr Prandtl number
Sr Soret number
T Temperature of the fluid
T_∞ Free stream temperature
a Stretching rate (constant)
g Acceleration due to gravity
G_r Thermal Grashof number
B_0 External magnetic field
Q_1' Dimensional radiation absorption parameter
Sh_x Sherwood number
J_w Wall heat flux
C_f Skin friction coefficient
Sc Schmidt number

Greek symbols

θ Non- dimensional temperature
μ_{nf} Dynamic viscosity of the nanofluid
v_f Kinematic viscosity of the base fluid
ρ_f Density of the nanofluid
κ_f Thermal conductivity of base fluid
ϕ Non dimensional concentration
σ Electrical conductivity
β_{nf} Coefficient of thermal expansion of the nanofluid

Sub scripts

f Base fluid
nf Nanofluid

1. Introduction

One of the necessaryparameters in heat transfer is that thermal conductivity of the operating fluid. Generally used fluids in heat transfer applications; such as water, ethylene glycol, and engine oil has low thermal conductivities, in comparison to thermal conductivities of solids, particularly metals. As a consequence, researchers have tried to seek out the way of rising thermal conductivity of those unremarkably used fluids. Initially, Choi and Eastman [1] presented the concept of nanofluids for suspension of liquids containing ultra-fine particles. Khan and Pop [2] in their first work on nanofluid have considered the problem of flow over astretching sheet. A numerical study ofmomentum, energy, and concentrationboundary layer flow has been performed by Makinde and Aziz [3]. Ibrahim et.al [4] analyzedthe MHD stagnation point flow and heat transfer due to nanofluid towards a stretching sheet by using Runge-kutta method fourth order method with shooting technique.Sheikholeslami et al. [5] consider CuO water and Al_2O_3 water nanofluid, and conclude with Nusselt number increases with theincrease of nanoparticle volume fraction. Kameswaran et al. [6] studied the two types of nanofluids namely silver oxide and copper oxide nanofluids. Turkyilmazoglu and Pop [7] studied heat and mass transfer of unsteady natural convection flow of different water-based nanofluids containing Cu, Ag, CuO, Al2O3, and TiO2 past a vertical infinite flat plate with radiation effect by using Laplace transform technique. Zhang et al. [8] investigated the MHD flow and radiation heat transfer of nanofluids in porous media with variable surface heat flux and chemical reaction. He also considered the three types of nanoparticles Cu, Al2O3 and Ag. Rana and Bhargava[9] studied the flow and heat transfer of a nanofluid over a nonlinearly stretching sheet. This problem was studied by using two methods namely finite element method and finite difference method. Nandy et al [10] numerically studied unsteady MHD boundary-layer flow and heat transfer of nanofluid over a permeable shrinking sheet in the presence of thermal radiation. Sudarsana Reddy et al [11] presented the heat and mass transfer flow of a nanofluid over an inclined plate under enhanced boundary conditions with themagnetic field and thermal Radiation by using finite element method. Chamkha and Aly [12] presented MHD free convection flow of a nanofluid past a vertical plate in the presence of heat generation or absorption effects. Bachok et al [13] studied flow and heat transfer characteristics on a moving plate in a nanofluid. Mahdi et al. [14] give the practical heat transfer process applications of

porous media with nanofluid.Loganathan et al. [15] studied theTransient natural convective flow of a nanofluid past a vertical plate in the presence of heat generation by Laplace transform technique also he studied skin friction and Nusselt number.

The current study is to analyze the results of chemically reacting on MHD boundary layer flow of CuO-water and MgO-water nanofluids past a stretching sheet in porous media with radiation absorption and heat generation/absorption. The governing partial differential equations are transformed into nonlinear ordinary differential equations by using similarity variables. The transformed equations were solved numerically by the shooting method with Runge-Kutta scheme.

2. Mathematical analysis

We consider the steady laminar two-dimensional MHD boundary layer flow of a viscous incompressible electrically conducting nanofluid over a stretching sheet through ananofluid-saturated porous medium in the presence of an applied magnetic field, chemical reaction, thermal radiation and radiation absorption as depicted in Fig. 1. The coordinate system x - axis is taken along the stretching surface in the direction of the motion and y -axis is normal to the flow direction. We also consider the influence of a constant magnetic field of strength B_0 which is applied normally to the plate. The surface of the plate is maintained at auniform temperature and concentration T_w and C_w these values are assumed to be greater than the ambient temperature and concentration T_∞ and C_∞ respectively. The flow is assumed to be confined to a region $y > 0$. In the present problem, the fluid is water- based nanofluid containing two different types of nanoparticles Silver (Ag) and Copper oxide (CuO). It is assumed that the fluid and nanoparticles are in thermal equilibrium and no slip occurs between them. The thermo physical properties of the nanofluid are given in table 1. Under the above assumptions the governing equations describing the momentum, energy, and concentration in the presence of thermal radiation, chemical reaction, Soret and Dufour effects taken the following form:

Table 1. Thermo- physical properties of water based nanoparticles:

Thermo physical properties	Base fluid (water)	CuO (Copper Oxide)	MgO (Magnesium Oxide)
$\rho(kg/m^3)$	997.1	6320	3580
$C_P(J/kg\,K)$	4179	531.8	960
$k(W/mK)$	0.613	76.5	48.4
$\beta\times10^5(K^{-1})$	21	1.80	1.26

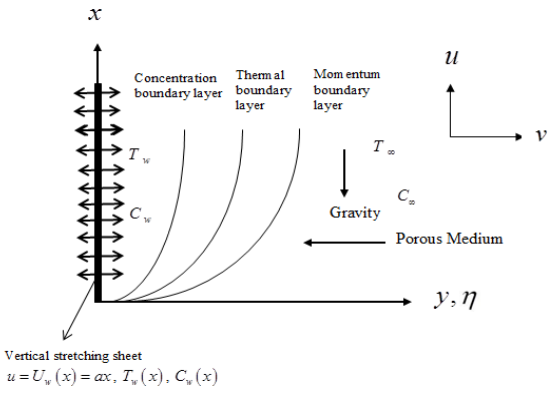

Figure1. Physical coordinate system

$$\frac{\partial u}{\partial x}+\frac{\partial v}{\partial y}=0 \tag{1}$$

$$u\frac{\partial u}{\partial x}+v\frac{\partial u}{\partial y}=\frac{1}{\rho_{nf}}\left[\mu_{nf}\frac{\partial^2 u}{\partial y^2}+g\left(\rho\beta\right)_{nf}\left(T-T_\infty\right)-\sigma {B_0}^2 u-\frac{\mu_{nf}}{k}u\right] \tag{2}$$

$$\begin{aligned}u\frac{\partial T}{\partial x}+v\frac{\partial T}{\partial y}=&\frac{k_{nf}}{\left(\rho C_P\right)_{nf}}\frac{\partial^2 T}{\partial y^2}-\frac{1}{\left(\rho C_P\right)_{nf}}\frac{\partial q_r}{\partial y}+\frac{\mu_{nf}}{\left(\rho C_P\right)_{nf}}\left(\frac{\partial u}{\partial y}\right)^2+\frac{Q_0}{\left(\rho C_P\right)_{nf}}\left(T-T_\infty\right)\\&+\frac{D_2}{\left(\rho C_P\right)_{nf}}\frac{\partial^2 C}{\partial y^2}+Q_1'\left(C-C_\infty\right)\end{aligned} \tag{3}$$

$$u\frac{\partial C}{\partial x}+v\frac{\partial C}{\partial y}=D_m\frac{\partial^2 C}{\partial y^2}+D_1\frac{\partial^2 C}{\partial y^2}-k_0\left(C-C_\infty\right) \tag{4}$$

The boundary conditions are

$$u=U_W\left(x\right)=ax, v=0,\ T=T_W,\ C=C_W \quad \text{at} \quad y=0$$

$$u\to 0,\ T\to T_\infty, C\to C_\infty \ \text{as}\ y\to\infty \tag{5}$$

Where u and v are the components of velocity along x and y directions respectively, g is the acceleration due to gravity, T is the temperature and C is concentration of the nanofluid, μ_{nf} is dynamic viscosity of the nanofluid, ρ_{nf} is density of the nanofluid, $\left(\rho C_P\right)_{nf}$ is heat capacitance of the nanofluid, D_m is species diffusivity, D_1 is mass flux through the temperature gradient, D_2 is heat flux through the concentration gradient, K is porous medium, k_0 is rate of chemical reaction, σ is the electrical conductivity, q_r is the radiative heat flux.

The flow is caused by the stretching of the sheet which moves in its own plane with the surface velocity $U_w(x)=ax$, where a (stretching rate) is positive constant. The dynamic viscosity μ_{nf}, density ρ_{nf}, heat capacitance $\left(\rho C_P\right)_{nf}$, thermal conductivity k_{nf} of the nanofluid and kinematic viscosity v_f of the base fluid are defined as follows:

$$\mu_{nf}=\frac{\mu_f}{\left(1-\varphi\right)^{2.5}},\ \rho_{nf}=\left(1-\varphi\right)_{\rho f}+\varphi\rho_s,\ \left(\rho C_P\right)_{nf}=\left(1-\varphi\right)\left(\rho C_P\right)_f+\varphi\left(\rho C_P\right)_s,$$

$$k_{nf}=k_f\left[\frac{k_s+2k_f-2\varphi(k_f-k_s)}{k_s+2k_f+\varphi(k_f-k_s)}\right] \tag{6}$$

The radiative heat flux is denoted by q_r. Using the Rosseland approximation for radiation, we have:

$$q_r = -\frac{4\sigma^*}{3K^*}\frac{\partial T^4}{\partial y} \tag{7}$$

Where σ^* the Stephan-Boltzman constant, K^* is the mean absorption coefficient. We assume that the temperature differences within the flow are such that the term T^4 may be expressed as a linear function of temperature. This is accomplished by expanding T^4 in a Taylor series about the free stream temperature T_∞ as follows:

$$T^4 = T^4{}_\infty + 4T^3{}_\infty (T - T_\infty) + 6T^2{}_\infty (T - T_\infty)^2 + \ldots\ldots\ldots\ldots \tag{8}$$

Omitting higher-order terms in the above equation (8) beyond the first degree in $(T - T_\infty)$, we get

$$T^4 \cong 4T^3{}_\infty T - 3T^4{}_\infty \tag{9}$$

Thus, substituting Eq. (9) into Eq. (7) we get

$$\frac{\partial q_r}{\partial y} = -\frac{16\sigma^* T^3{}_\infty}{3k*}\frac{\partial^2 T}{\partial y^2} \tag{10}$$

Therefore equation (3) reduced to

$$u\frac{\partial T}{\partial x} + v\frac{\partial T}{\partial y} = \frac{k_{nf}}{(\rho C_P)_{nf}}\frac{\partial^2 T}{\partial y^2} + \frac{1}{(\rho C_P)_{nf}}\frac{16\sigma^* T^3{}_\infty}{3k*}\frac{\partial^2 T}{\partial y^2} + \frac{\mu_{nf}}{(\rho C_P)_{nf}}\left(\frac{\partial u}{\partial y}\right)^2 + \frac{Q_0}{(\rho C_P)_{nf}}(T - T_\infty) + \frac{D_2}{(\rho C_P)_{nf}}\frac{\partial^2 C}{\partial y^2} + Q_1'(C - C_\infty) \tag{11}$$

The following similarity transformations are introduced to simply the mathematical analysis of the problem

$$u = axf'(\eta),\ v = -\sqrt{av_f}\,f(\eta),\ \eta = \sqrt{\frac{a}{v_f}}\,y,\ \theta(\eta) = \frac{T - T_\infty}{T_W - T_\infty},\ \phi(\eta) = \frac{C - C_\infty}{C_W - C_\infty} \tag{12}$$

Using Equations (11) and (12) the governing non-linear partial differential equations (1-4) together with the boundary condition (5) reduce to first ordinary differential equations.

Momentum boundary layer equation:

$$f''' + A_1A_3Gr\theta - MA_1f' - Kf' - A_1A_2\left(f'^2 - ff''\right) = 0 \tag{13}$$

Thermal boundary layer equation:

$$A_1 A_5\left(1+\frac{4}{3N}\right)\theta'' + \Pr Ecf''^2 + A_1 \Pr Q\theta + A_1 \Pr Du\phi'' + A_1 A_4 \Pr f\theta' + A_1 A_4 \Pr \phi Q1 = 0 \quad (14)$$

Concentration boundary layer equation:

$$\phi'' + Scf\phi' + SrSc\theta'' - kSc\phi = 0 \quad (15)$$

The transformed boundary conditions are

$$\eta = 0\ f = 0,\ f' = 1,\ \theta = 1,\ \phi = 1$$

$$\eta \to \infty\ f' = 0, \theta = 0, \phi = 0 \quad (16)$$

Where $Gr = \frac{g\beta_f (T_W - T_\infty)}{au}$ is the buoyancy parameter, $M = \frac{\sigma B_0{}^2}{\rho_f a}$ is the magnetic parameter, $K = \frac{\mu_f}{ak\rho_f}$ is the Porous medium parameter, $\Pr = \frac{\mu_f (Cp)_f}{k_f}$ is the Prandtl number, $N = \frac{k_{nf} k^*}{4\sigma^* T_\infty{}^3}$ is the radiation parameter, $Ec = \frac{u^2}{(Cp)_f (T_W - T_\infty)}$ is the Eckert number, $Q = \frac{Q_0}{a(\rho Cp)_f}$ is the heat generation, $\psi = \frac{Q_1 (C_W - C_\infty)}{a(T_W - T_\infty)}$ is the radiation absorption, $Sr = \frac{D_1 (T_W - T_\infty)}{v_f (C_W - C_\infty)}$ is the Soret number, $Du = \frac{D_2 (C_W - C_\infty)}{v_f (\rho Cp)_f}$ is the Dufour number, $Sc = \frac{v_f}{D_m}$ is the Schmidt number, $k = \frac{k_0}{a}$ is the chemical reaction parameter.

$$A_1 = (1-\varphi)^{2.5},\quad A_2 = (1-\varphi) + \varphi\left(\frac{\rho_s}{\rho_f}\right),\quad A_3 = (1-\varphi) + \varphi\left[\frac{(\rho\beta)_s}{(\rho\beta)_f}\right],\quad A_4 = (1-\varphi) + \varphi\left[\frac{(\rho C_P)_s}{(\rho C_P)_f}\right],$$

$$A_5 = \frac{k_{nf}}{k_f}$$

Quantities of physical interest are the local skin friction coefficient C_{fx} the local Nusselt number N_{ux} and the local Sherwood number Sh_x, which can be expressed as:

$$C_{fx} = \frac{\tau_{wx}}{\rho_f U_w^2},\ N_{ux} = \frac{xq_w}{k_f (T_w - T_\infty)},\ Sh_x = \frac{xq_m}{D_B (C_w - C_\infty)} \quad (17)$$

Here τ_{wx} is the wall shear stress and q_w and q_m are the surface heat and mass fluxes, respectively, which are defined as:

$$\tau_{wx} = \mu_{nf}\left(\frac{\partial u}{\partial y}\right)_{y=0},\ q_w = -k_{nf}\left(\frac{\partial T}{\partial y}\right)_{y=0},\ q_m = -D_B\left(\frac{\partial C}{\partial y}\right)_{y=0} \quad (18)$$

Substituting (12) into (17) and using equation (18), we obtain

$$\frac{1}{2}C_{fx}\,\mathrm{Re}_x^{1/2} = \frac{f''(0)}{(1-\varphi)^{2.5}} \tag{19}$$

$$Nu_x\,\mathrm{Re}_x^{-1/2} = -A_5\left(1+\frac{4}{3N}\right)\theta'(0) \tag{20}$$

$$Sh_x\,\mathrm{Re}_x^{-1/2} = -\phi'(0) \tag{21}$$

3. Results and Discussion

This work is concerned with the study of MHD free convective boundary layer flows of nanofluids past a uniformly stretching sheet through porous media with radiation absorption, heat generation/absorption, thermal radiation, chemical reaction, thermo-diffusion and diffusion –thermo effects.The physical effects of nanoparticles on the velocity, the temperature and the concentration profiles as well as on the skin friction coefficient, the local Nusselt number and Sherwood number are discussed numerically. We have consider M=2, Pr=6.8, N=4, Ec=0.1, K1=1, Gr=10, Du=0.5, Sr=0.5, Sc=1, Kr=0.5, Q= -0.1 and Q1=0.5. In order to get the physical signs of the flow and the heat transfer characteristics are plotted in Figs. (2-17).the effect of the magnetic field parameter (M) on the velocity profile is shown in Fig.2 for both CuO-water and MgO –water based nanofluids. From Fig.2 it is found that the velocity is declining in growing the magnetic field parameter. This is due to that the drag force. It is prominent to mention here that magnetic field effect is highly significant on MgO–water nanofluid while compared with CuO–water nanofluid. Figs (3-4) show the effect of nanoparticle volume fraction φ on the nanofluid velocity and temperature respectively. It can be observed that with an increase in the volume fraction of the nanoparticles decreases the velocity and increases the temperature and concentration profiles of both CuO–water, and MgO–water nanofluids. It is due to the fact that an increase in the volume fraction improves the density of the nanofluid and it causes to slowdown the fluid velocity and improves the thermal conductivity. Further, we also observe that the CuO–water based nanofluid displayscomparatively less velocity than that of the MgO–water based nanofluid in the velocity profile, but in the temperature and concentration distribution, the CuO–water based nanofluid is greater than that of the MgO –water based nanofluid. These figures show the goodarrangement with the physical behaviour.

The effects of heat generation/ absorption and radiation absorption on the velocity and temperature profiles are shown in Fig. 5 and 6, respectively for both CuO –water, and MgO –water based nanofluids. It is obvious that the velocity and temperature increase with an increase in the heat source parameter. These results qualitatively agree with expectancy since the effect of internal heat generation is to increase the rate of heat transport to the fluid thereby increasing the velocity of the fluid and also increasing its temperature, we also observe that an increase the radiation absorption parameter the nanofluid velocity and temperature increases for both the fluids is presented in Fig. 7 and 8. It is interesting to note that copper oxide nanofluid has effective thermal conductivity while compared with magnesium oxide nanofluid, but the reverse phenomena is found in the velocity profile. The velocity and temperature profiles are shown in Figs (9-10) for different values of Prandtl number. It was noticed that the both velocity and temperature profiles are decreases with increasing Prandtl number for both the nanofluids. By the definition, the Prandtl number is defined as the ratio of the momentum diffusivity to the thermal diffusivity and therefore, increasing the values of Prandtl number means higher momentum diffusivity or lesser thermal diffusivity which causes the reduction in the thermal boundary layer thickness and this deceleration in the temperature profiles is higher in the CuO –water nanofluid than the MgO –water nanofluid Fig 10.

The velocity, temperature and concentration profiles of the CuO –water and MgO –water nanofluids for different values of the Dufour and Soreteffects are depicted in Figs. 11-15. It is observed that the velocity in the momentum boundary layer, temperature boundary layer and concentration boundary layer increases with the increasing values of Dufour and Soret effect parameters, we also observe that in Fig. 13 that increasing the values of Dufour parameter (Du) reduce the concentration in the fluid flow for both the nanofluids. Fig. 16 exhibits the effect of porous media on the velocity field. From this figure, it is observed that an increase porous media (K1) increases the velocity for both nanofluids. The concentration profile for different values of Schmidt number is presented in Fig. 17. It is observed that increase of Schmidt number leads to the decrease in concentration of the species.

From table.2 it is interesting to note that magnesium oxide nanofluid has effective thermal conductivity while compared with copper oxide nanofluid in the rate of heat transfer, but in the skin friction copper oxide nanofluid is higher than magnesium oxide nanofluid. The skin friction coefficient increases with the increasing values of M and N. and decreases with Q1,Q,Du,Sr. the reduced Nusselt number decreases with Q1,Q,Du,Sr and also the Sherwood number is increasing for increases Du,Sr,Kr,Sc. It is found that the skin friction is decreased for increasing nanoparticle volume fraction is increasing, but the reverse effect will be found in Nusselt number.

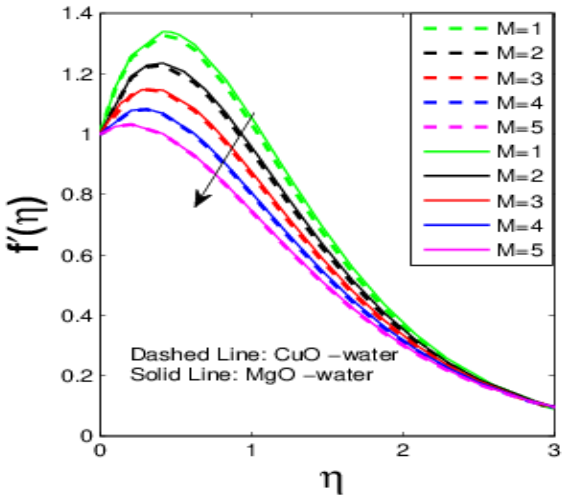

Figure 2. Effect of M on $f'(\eta)$

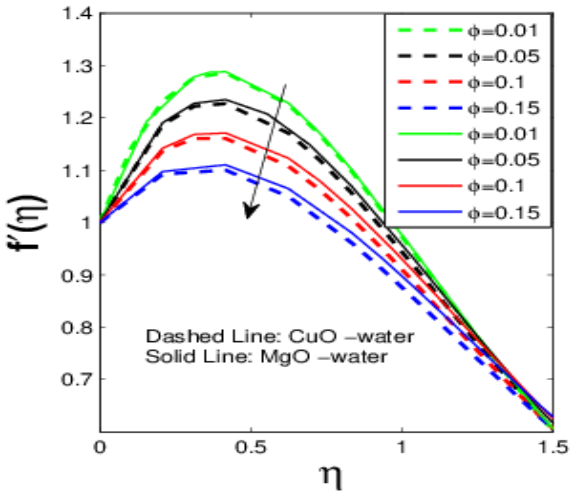

Figure 3. Effect of φ on $f'(\eta)$

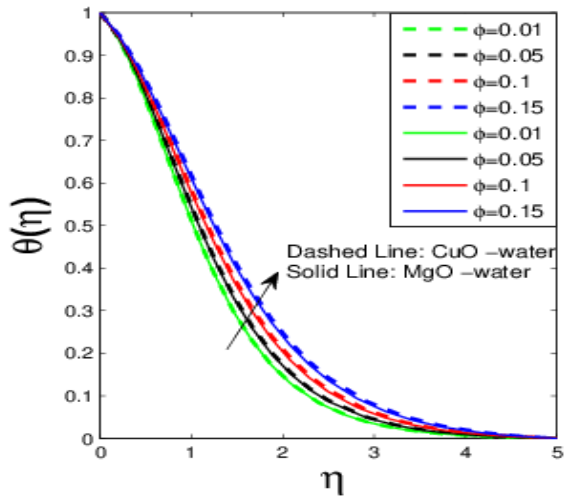

Figure 4. Effect of φ on $\theta'(\eta)$

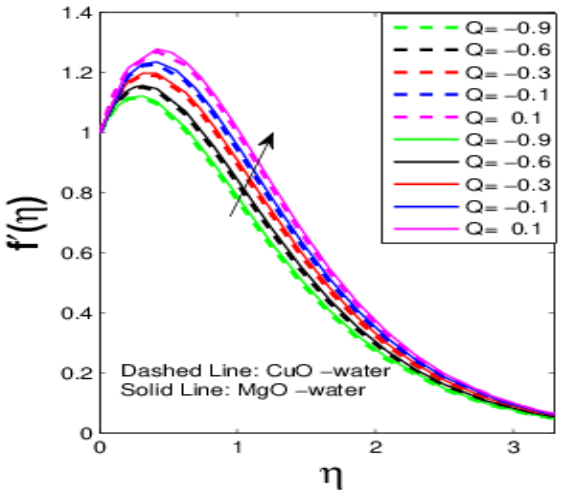

Figure 5. Effect of Q on $f'(\eta)$

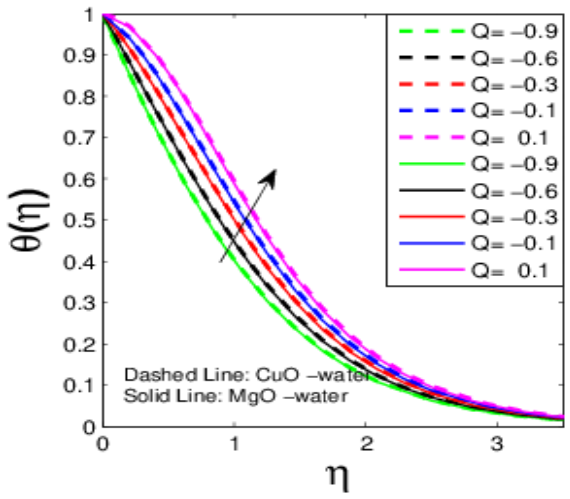

Figure 6. Effect of Q on $\theta'(\eta)$

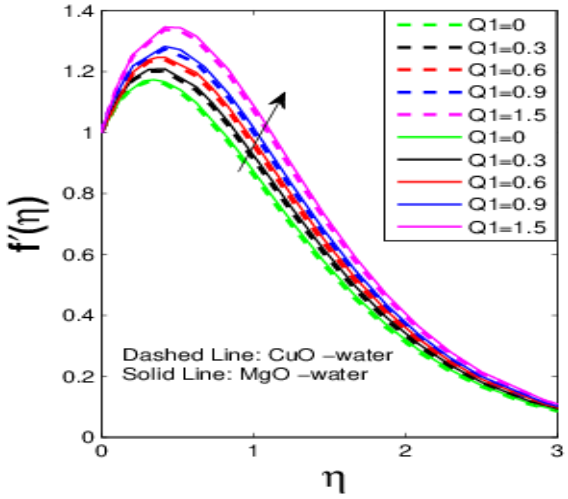

Figure 7. Effect of $Q1$ on $f'(\eta)$

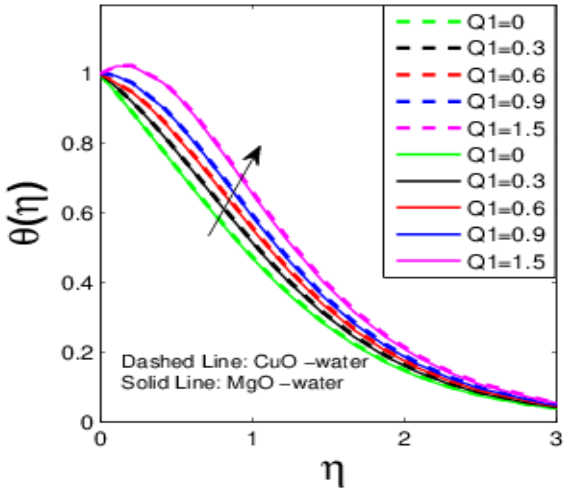

Figure 8. Effect of $Q1$ on $\theta'(\eta)$

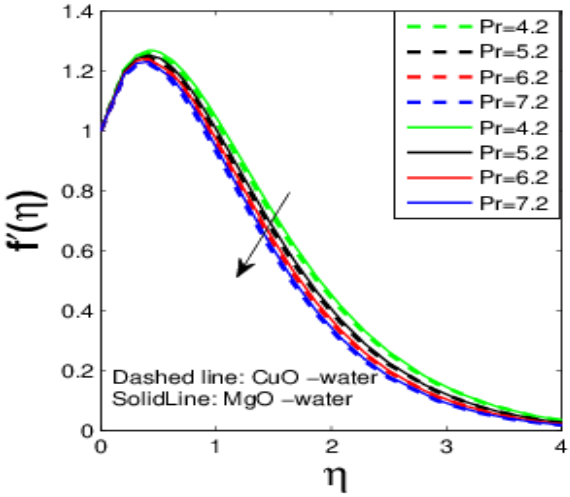

Figure 9. Effect of $\Pr$ on $f'(\eta)$

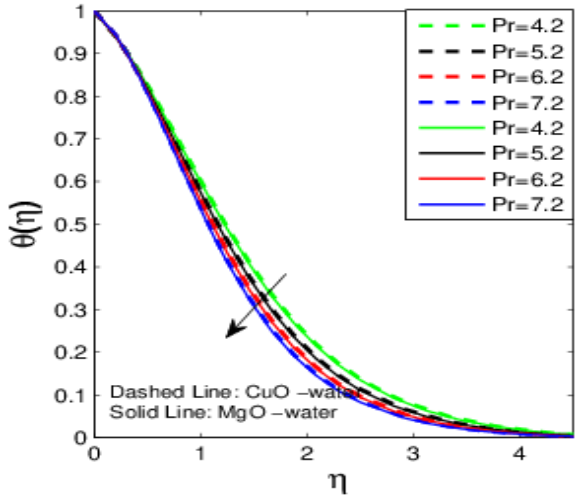

Figure 10. Effect of $\Pr$ on $\theta(\eta)$

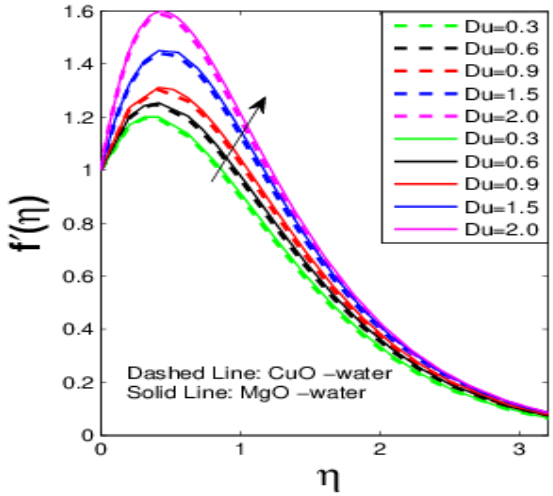

Figure 11. Effect of Du on $f'(\eta)$

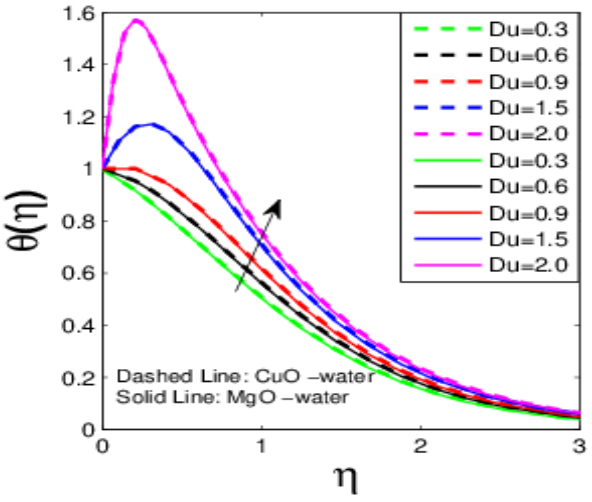

Figure 12. Effect of Du on $\theta(\eta)$

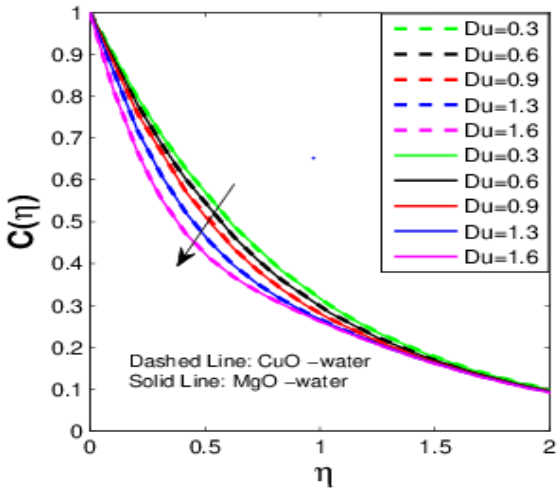

Figure 13. Effect of Du on $C(\eta)$

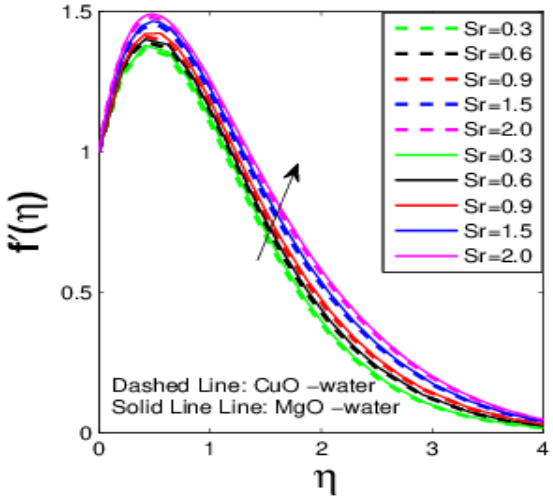

Figure 14. Effect of Sr on $f'(\eta)$

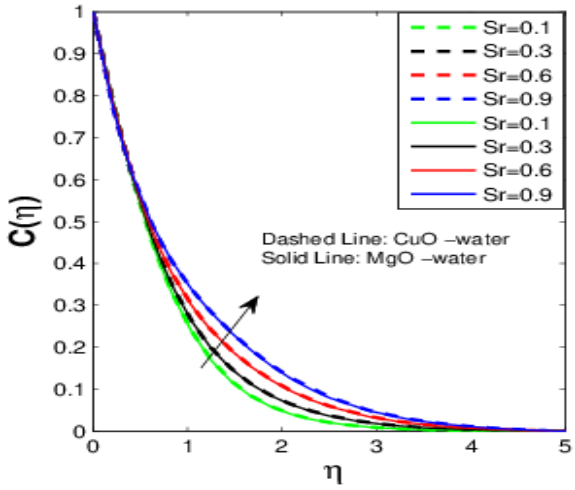

Figure 15. Effect of Sr on $C(\eta)$

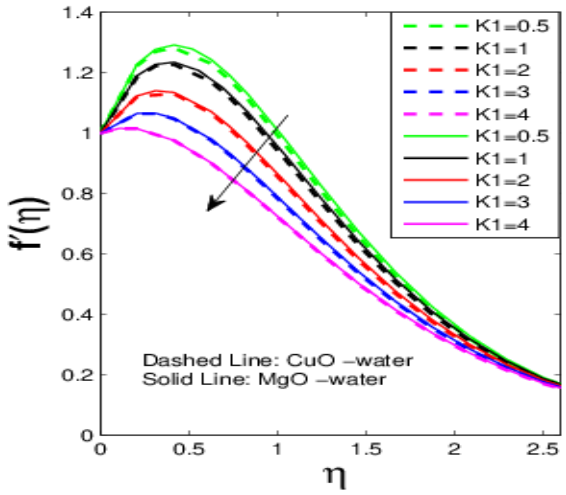

Figure 16. Effect of $K1$ on $f'(\eta)$

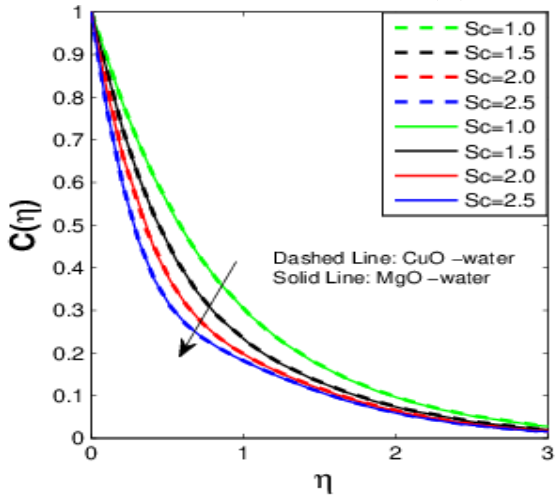

Figure 17. Effect of Sc on $C(\eta)$

Table 2.

Parameter		Skin friction $-f''(0)$		Nusselt number $-\theta'(0)$		Sherwood number $-\phi'(0)$	
		CuO	*MgO*	*CuO*	*MgO*	*CuO*	*MgO*
M	0.5	1.376	1.334				
	1.0	1.526	1.488				
	1.5	1.663	1.627				
	2.0	1.789	1.757				
N	1	1.785	1.752	-1.734	-1.72		
	2	1.788	1.755	-0.7081	-0.0699		
	3	1.789	1.756	-0.4056	-0.3998		
	4	1.789	1.757	-0.2571	-0.2526		
Q	-0.9	1.801	1.768	0.5237	0.5273		
	-0.6	1.798	1.765	0.2952	0.2988		
	-0.3	1.794	1.761	0.0033	0.00725		
*Q*1	0.1	1.783	1.750	-0.6292	-0.6234		
	0	1.795	1.762	0.1592	0.1642		
	0.3	1.792	1.759	-0.0982	-0.0935		
	0.6	1.788	1.756	-0.3331	-0.3288		
	0.9	1.785	1.743	-0.5492	-0.5454		
Du	0	1.794	1.761	0.09977	0.1046	0.9442	0.9442
	0.3	1.791	1.791	-0.0979	-0.09335	1.024	1.024
	0.6	1.788	1.788	-0.3473	-0.343	1.126	1.126
	0.9	1.755	1.785	-0.6771	-0.6733	1.266	1.266
Sr	0.3	1.79	1.757	-0.2155	-0.211	0.994	0.9948
	0.6	1.789	1.756	-0.2808	-0.2764	1.144	1.143
	0.9	1.789	1.755	-0.3688	-0.3645	1.349	1.347
	1.5	1.787	1.755	-0.7137	-0.7102	2.150	2.147
Kr	1					1.378	1.378
	2					1.811	1.811
	3					2.153	2.153
	4					2.445	2.445
Sc	1					1.089	1.089
	1.5					1.487	1.487
	2					1.941	1.94
	2.5					2.51	2.511
φ	0	1.817	1.817	-0.3322	-0.3322		
	0.05	1.789	1.757	-0.2571	-0.2526		
	0.1	1.752	1.693	-0.1968	-0.1894		
	0.2	1.651	1.556	-0.1062	-0.0956		

4. Conclusions

In the recent study, chemically reacting on MHD boundary layer flow of CuO-water and MgO-water nanofluids past a stretching sheet in porous media with radiation absorption and heat generation/absorption.The governing partial differential equations are formulated into ordinary differential equations with the help of similarity transformation and variables. And being solved numerically by using Runge- Kutta method with shooting technique. The authors have examined the following outcomes from the model:

- The velocity profiles of CuO–water and MgO–water based nanofluids are reduced as accelerating in magnetic field parameter, theporosity of the medium.
- The momentum boundary layer and concentration boundary layer reduces as anincrease in nanoparticles volume fraction, but energy boundary layer is increased for both the nanofluids.
- Both the velocity and temperature profiles increase with increasing the values of radiation absorption and heat generation parameter for both the nanofluids.
- The nanofluid velocity and temperature increases with increasing Dufour parameter where as it is noticed that the opposite reactions in concentration field.
- For the Prandtl number increases both the velocity and temperature is decreased.
- The concentration and velocity areincreased for increasing Soretparameter, we also noticed that the concentration is decreased for increasing the Schmidt number.
- The skin-friction coefficient and Nusselt number are decreases for increasing Q1, Q, Du, Sr in both the fluids.
- Interesting to see in our study of copper oxide nanofluid have less velocity than the magnesium oxide nanofluid, but in quite opposite that magnesium oxide nanofluid is higher than the copper oxide nanofluid in heat transfer.

References

[1] Choi SUS, Eastman JA 1995 *ASME, San Francisco, USA, FED 231/MD***66** 99–105
[2] Khan WA, Pop I 2010 *Int. J Heat Mass Transfer***53** 2477–2483
[3] Makinde O D, Aziz A 2011 *Int. J Thermal Sciences***50(7)** 1326–1332
[4] Ibrahim W, Shankar B, and Nandeppanavar M.M 2013 *Int. J Heat and Mass Transfer* **56**(1-2) 1–9
[5] Sheikholeslami M, Abelman S, and Ganji D. D 2014 *Int. J Heat and Mass Transfer* **79** 212–222
[6] Kameswaran PK, Narayana M, Sibanda P, and Murthy P V S N 2012 *Int. J Heat and Mass Transfer***55**(25-26) 7587–7595
[7] Turkyilmazoglu M, Pop I 2013 Int. J Heat Mass Transfer 59 167–171
[8] Zhang C, Zheng L, Zhang X, and Chen G 2015 *Appl Math Modell***39** 165–181
[9] RanaP,andBhargava R 2012 *A numericalstudycommun. NonlinearSci. Numer. Simul.***17** 212-226
[10] Samir Kumar Nandy, SumantaSidui, and Tapas Ray Mahapatra 2014 *Alexandria Engineering Journal*. **53**(4) 929-937
[11] Sudarsana Reddy P, Sreedevi P, and Chamkha AJ 2016 *Heat Transfer-Asian Research*
[12] Chamkha A J, and Aly A M 2010 *Chemical Engineering Communications***198** (3) 425-441
[13] Bachok N, Ishak A, Pop I 2012 *Int. J. Heat Mass Transfer***55** 642–648
[14] Raed Abed Mahdi, Mohammed H.A, Munisamy K.M, and Saeid N.H 2015 Renewable and SustainableEnergyReviews 41 715-734
[15] Loganathan P, Nirmal Chand P, Ganesan P 2015 *Journal of AppliedMechanics and TechnicalPhysics***56**(3) 433-442